

# Spiral and concentric waves organize multicellular *Dictyostelium* mounds

Florian Siegert and Cornelis J. Weijer

Zoologisches Institut, Universität München, Luisenstrasse 14, 80333 München 2, Germany.

**Background:** It has been known for more than 20 years that the early aggregation of the slime mould *Dictyostelium* is driven by periodic waves of cAMP, which instruct the cells to collect at the aggregation centre. Although it has been hypothesized that cAMP waves are also involved in the organization of multicellular morphogenesis, wave propagation in the later stages of *Dictyostelium* development has not previously been demonstrated.

**Results:** We have developed special optical and digital-image-processing techniques that allow propagating waves of chemotactic activity to be visualized in multicellular aggregates. Using this technology, we have observed signal propagation in the multicellular, 'mound' stage of *Dictyostelium discoideum*. Within mounds, these waves were propagated as concentric rings, single armed spirals or multi-armed spirals. The spontaneous appearance of the latter structures was new and unexpected. The geometry

of wave propagation was strain specific: strain XP55 predominantly showed concentric ring waves, whereas spiral waves were typical of a derivative of XP55, streamer F mutant NP377, and of the widely used axenic strain AX-3. The different geometry of the signals was reflected by distinct cell-movement patterns and different cell-movement speeds — cells in AX-3 mounds, organized by spiral waves, moved faster than cells in XP55 mounds, and spiral waves were always accompanied by rotational cell movement, whereas cells in XP55 mounds moved towards the aggregation centre.

**Conclusions:** The same principles — wave propagation and chemotaxis — that control *Dictyostelium* aggregation also govern the morphogenesis of the mound stage. Mounds behave as a highly excitable system in which a diverse range of signal-propagation geometries create the same biological structure — a migrating slug.

Current Biology 1995, 5:937–943

## Background

In biology, *de novo* pattern formation is most prominent during embryogenesis. It involves the spatio-temporal control of cell differentiation, as well as of differential cell movement. Our experiments have addressed the role of differential cell movement in the morphogenesis of a simple system, the cellular slime mould *Dictyostelium discoideum*. This organism exists in both single and multicellular forms in different phases of its life cycle. In the vegetative stage, cells live as solitary amoebae and feed on bacteria; under starvation conditions, thousands of amoebae chemotactically aggregate to form a simple fruiting body that consists of stalk and spore cells (Fig. 1).

The aggregation of individual *Dictyostelium* amoebae requires cell-to-cell communication and coordinated cell movement. Aggregation occurs by chemotaxis in response to periodic cAMP signals, initiated by the aggregation centre, which are detected, amplified and relayed by the surrounding cells (reviewed in [1]). This leads to an outward propagation of the cAMP waves. Chemotaxis in the direction of increasing cAMP concentration leads to the formation of streams, and ultimately to multicellular aggregates.

During early aggregation, cAMP wave propagation can be seen as optical-density wave propagation using low-power darkfield optics [2,3]. These optical-density waves

are correlated with shape changes which cells undergo upon stimulation with cAMP — chemotactically moving cells are elongated and appear brighter than non-moving cells. The optical-density waves therefore represent the propagating cAMP signal [4]. During aggregation, waves appear most often as expanding spirals, although concentric ring waves are seen in some strains (Fig. 1) [5]. Quantitative measurements of several parameters of these propagating darkfield waves have shown that cAMP-wave propagation can be described in terms of a mathematical theory that was developed to describe the well-known Belousov-Zhabotinsky chemical reaction [6].

Bifurcating aggregation streams, in which propagating waves are still visible, are formed later during aggregation. Stream formation has been shown to result from a dependence of the rate of wave propagation on cell density (C. Van Os, A.V. Panfilov, P. Hogeweg, F.S. and C.J.W., unpublished observations). The cells in the streams move toward the aggregation centre and collect in a hemispherical cell mass — the mound. During the mound stage, the cells start to differentiate into two distinct types — the prestalk and prespore cells — which later form the stalk and spore head of the fruiting body [7]. The prestalk cells differentiate at random positions within the mound, but later become sorted to form a tip on top of the mound structure. This tip guides all further developmental processes, and it was therefore attributed the role of an embryonic organizer [8].

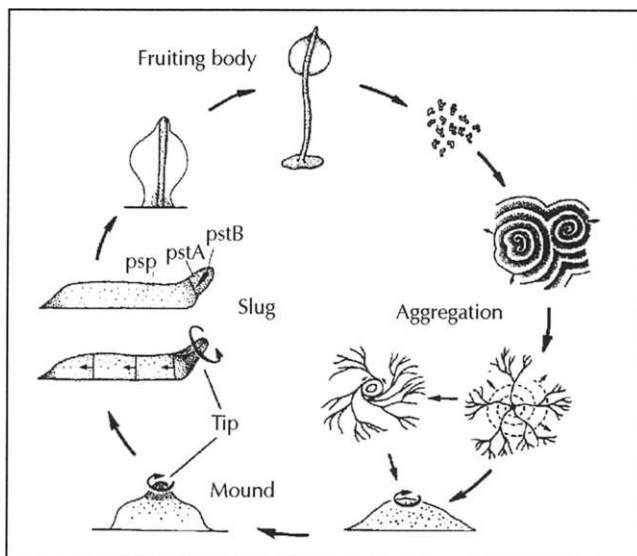


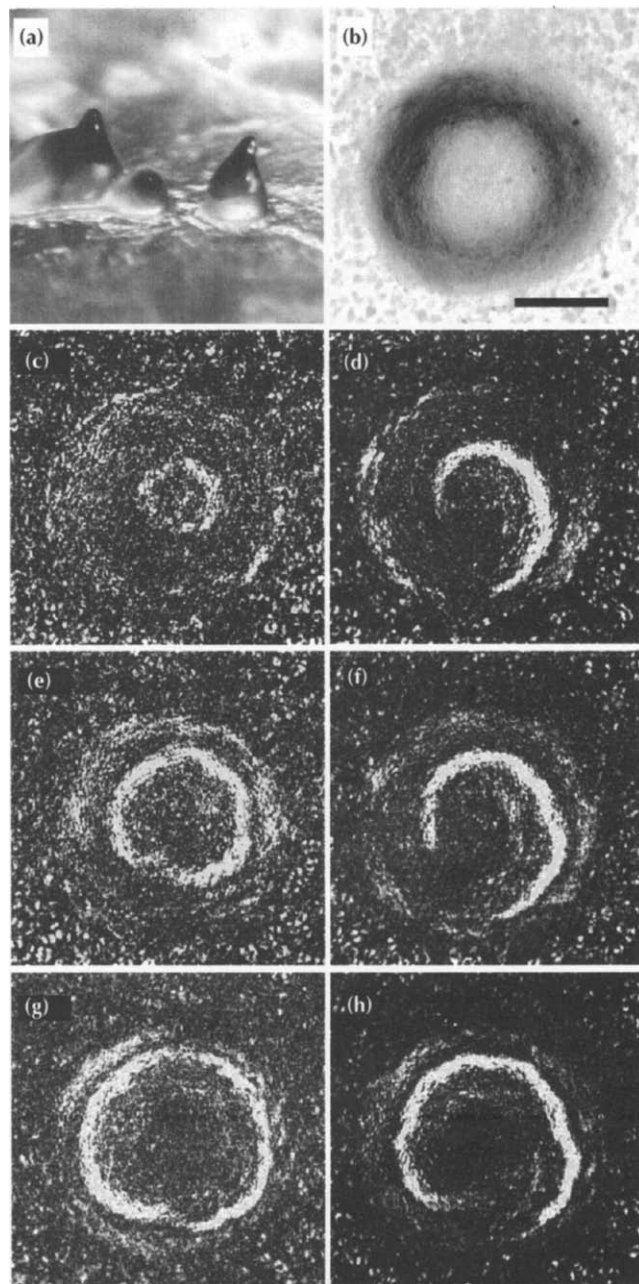
**Fig. 1.** Life-cycle of the cellular slime mould *Dictyostelium discoideum*. Upon starvation, single cells begin to move chemotactically towards an aggregation centre. The chemotactic signal is visible as an expanding optical-density spiral originating from the aggregation centre. After about 20 waves, cells collect in bifurcating aggregation streams and finally form a hemispherical cell mass, the mound. In the mound, the cells differentiate at random into at least three types: prespore cells (psp) and two pre-stalk cell types (pstA, pstB). The prestalk cells sort chemotactically to the top of the mound and form the tip. In the slug tip, the pstB cells form a funnel-shaped structure, from which the stalk develops. The pstA cells surround the pstB cells. The tip directs morphogenesis until fruiting-body formation. Circular arrows indicate the direction of wave propagation.

As periodic cAMP signals control development from early aggregation until stream formation, we investigated whether such signals also control multicellular development during the mound stage. We have developed special optical and image-processing techniques to visualize optical-density wave propagation in mounds. Here, we characterize the dynamics and geometry of these waves.

## Results

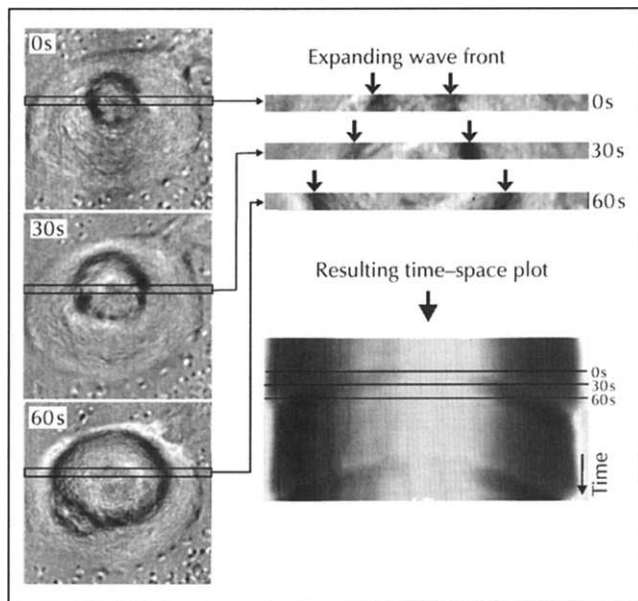
### Spatial behaviour of wave propagation: concentric rings and spiral waves

Figure 2a shows a side-view of three mounds at different stages of development; each mound consists of  $10^3$ – $10^5$  individual cells. In our experiments, mounds were observed through the agar with the microscope focused on the agar surface (Fig. 2b). Under appropriate illumination and magnification, chemotactic movement and wave propagation could be observed continuously, from early aggregation until the formation of mounds, using darkfield optics. Video images were stored in time-lapse mode on an optical disc recorder and later evaluated by digital-image processing. Optical-density waves are invisible in a single video frame — only time-lapse recordings with 240-fold time compression allow the identification of the weak optical-density signal. We therefore visualized the waves by an image-subtraction algorithm. In the resulting image,



**Fig. 2.** Wave propagation in mounds. (a) Side view of three typical mounds. Different stages of mound formation are visible. Two of the mounds have formed tips, whereas the centre mound is less developed. (b) Darkfield image (bottom view) of an XP55 mound. Scale bar = 100  $\mu\text{m}$ . (c,e,g) Circular wave propagation in the mound shown in (b). Four images were stored at 25 s intervals ( $t = 0, 25, 50$  and  $75$ ). Wave propagation was visualized by an image-subtraction algorithm — the subtraction of two darkfield images showing propagating darkfield waves results in bright pixel values where the two images differ and dark values where the two images are identical. (c) Image obtained by subtracting image  $t = 25$  from image  $t = 0$ . (d) Image  $t = 50$  subtracted from image  $t = 25$ . (e) Image  $t = 75$  subtracted from image  $t = 50$ . (d,f,h) Spiral-wave propagation in the same mound 15 min later (time scale and analysis as above).

the propagating wave appeared white on a dark background and, due to a slight rotational movement of the whole mound, the outlines of the mound became visible.



**Fig. 3.** Construction of time–space plots. The three images to the left show successive time points of an expanding concentric ring wave in an XP55 mound. The waves were visualized by subtracting successive video images from an initial image. The results of successive subtractions were then summed-up. This allows the visualization of the otherwise invisible leading-edge of the dark-field wave as a black concentric ring wave. The intensity values within the indicated window (500 pixels long, 20 pixels high) were averaged over the heights in order to reduce the two-dimensional image information at each time point to a single line of intensity values (500 pixels long). These lines obtained at successive time were placed below each other, resulting in a time–space plot (lower right panel). The x-axis in this time–space plot represents the length of the window, and the y-axis represents time. The position of the lines obtained from the three windows shown are indicated by black lines in the plot.

Figure 2c,e,g show an expanding concentric ring wave in an XP55 mound. Figure 2d,f,h show the same mound 15 minutes later, with a rotating spiral wave propagating counter-clockwise. The spiral was formed from the concentric ring wave by symmetry breaking. As can be seen in Figure 2e,g, the bottom part of the wavefront showed an indentation which enlarged over time. Not all cells along the path of the expanding concentric ring were able to propagate the cAMP signal at the same velocity. As a consequence, the ring became increasingly deformed during the propagation of additional waves, until it fragmented and two open ends formed. One end curved towards the pulsatile centre, forming a spiral wave that rotated around the organizing centre; the other end drifted to the outer edge of the mound and disappeared. After two rotations, the spiral tip drifted to the periphery and concentric ring waves reformed again. Such transitions were observed several times within individual mounds over the course of one hour.

#### Temporal dynamics of wave propagation

In order to quantify wave propagation in mounds over time, we constructed time–space plots by measuring changes in optical density along the cross-section of a mound [3]. Time–space plots allow the detection of very

weak signals that cannot be detected by the image-subtraction method. Figure 3 shows the construction of a time–space plot from a time-series of video images. First, an averaged intensity profile along the centre of the mound was calculated. Such lines were stored for many successive time points during the experiment. Second, these intensity profiles were placed below each other; in the resulting image, the x-axis represents the original length of the window and the y-axis indicates time. A circular optical-density wave, originating from a point-source in the middle of the mound and expanding until it reaches the outer border of the mound, appears in time–space plots as a ‘roof-shaped’ line structure. If the propagation speed stays constant, the slope of these lines is also constant. By measuring the steepness of the slope it is possible to determine the velocity of wave propagation. Steep slopes indicate low velocities, whereas flat slopes indicate high velocities. An intensity profile along the time axis also allows analysis of the period length between successive waves.

Figure 4a–d show a typical time–space plot of an XP55 mound measured over 3.5 hours. Under darkfield illumination, waves that originated in the centre of the mound and propagated towards the periphery were observed as a pattern of closely-spaced, alternating dark and bright bands. Upon stimulation with cAMP, *Dictyostelium* amoebae contract (the ‘cringe response’) before they start to move chemotactically [9]. This could be seen as a sharp minimum peak in the intensity plots (Fig. 4g,h). The mound contracted during the measurement; this was indicated by a decrease in the cross-section of the mound in the time–space plot (x-axis in Fig. 4a–d). During this contraction process, the mound extended up into the air and a tip formed in the middle. Tip formation, visible in Figure 4d, changed the optical properties of the mound such that further measurements of darkfield waves were impossible.

By determining the slope of the bands, we found that the wave-propagation velocity decreased from  $120 \mu\text{m min}^{-1}$  to  $60 \mu\text{m min}^{-1}$  during the time of observation. By measuring the distance between successive bands, we also found that the oscillation period of the darkfield waves decreased from 15 minutes to 2.5 minutes. Such a wide range of periods was found only in mounds organized by concentric ring waves. Furthermore, in XP55, a pronounced ‘beating’ behaviour was observed — some waves led to more vigorous contractions than others. This is visible in Figure 4c: four bands appeared slightly more intense. Between two such strong pulses, two or three weaker oscillations appeared.

Figure 4e shows a typical time–space plot of a mound of the streamer F mutant NP377, a derivative of XP55 [10], which is organized by spiral waves. Spiral-wave propagation could be identified in this plot as the rotating tip caused a dark ‘zigzag’ pattern in the centre of the mound. Due to the rotational cell movement, the mound was driven slightly to the left. The spiral waves observed

in NP377 do not appear to be caused by the streamer phenotype, as these waves were also observed in the widely-used non-streaming strain AX-3.

Mounds organized by spiral centres always showed oscillations at a higher frequency than mounds of strain XP55. The oscillation period (the time between oscillations) in these mounds was found to be 3 minutes at the end of the aggregation, and decreased further to 2 minutes at the time of tip formation (note that the time-scale in Figure 4e is different to that of Figure 4a–d). Figure 4f,g show a direct comparison of the period lengths of XP55 and NP377. NP377 produced nine waves in 20 minutes, whereas XP55 initiated only three waves in this time period. Figure 4h shows the decrease of the period length during the the whole sequence of mound formation in XP55 (note negative spikes).

Table 1 shows a quantitative comparison of several parameters related to signal propagation, measured during several independent experiments in XP55 and AX-3 mounds. On average, the oscillation period in AX-3 mounds was half that in XP55 mounds. Furthermore, in AX-3 mounds, the velocity of signal propagation was double that of XP55. Both strains showed consistently different patterns of signal propagation: XP55 was predominantly organized by concentric ring waves, whereas AX-3 always showed spiral waves. This strain-specific behaviour may be correlated to a genetically determined difference in the ability of the cells to generate and relay the cAMP signal.

### Mounds organized by several pacemakers

We often observed more complicated modes of wave propagation. The images in Figure 5 were obtained by a modified image-subtraction algorithm, which gave better results for complex wave patterns. Successive video images were subtracted from a reference image at the beginning of the time-series, as described above. However, in this case, the resulting subtraction images were added over time. Bright pixel values indicate the expanding optical density wave (note also the movement of single cells surrounding the mound). Figure 5a,b show an XP55 mound which was temporarily organized by two autonomously oscillating centres. Concentric rings originated from both centres and expanded through the mound. At the point where the two wavefronts meet in the middle of the mound they extinguished each other — a diagnostic property of an excitable medium [11].

Figure 5c,d show a mound which was organized by three autonomously oscillating centres. In large mounds, as many as five centres were observed simultaneously producing concentric rings (data not shown). The overall periodicity was nearly equal, but the rings appeared at slightly different times and in different and changing positions. Ultimately, only one centre survived.

### Multi-armed spirals

In strain AX-3, we routinely observed multi-armed spirals at a particular stage of development; this is the first observation of such spirals in *Dictyostelium*. Figure 6a shows a mound under darkfield illumination, and Figure

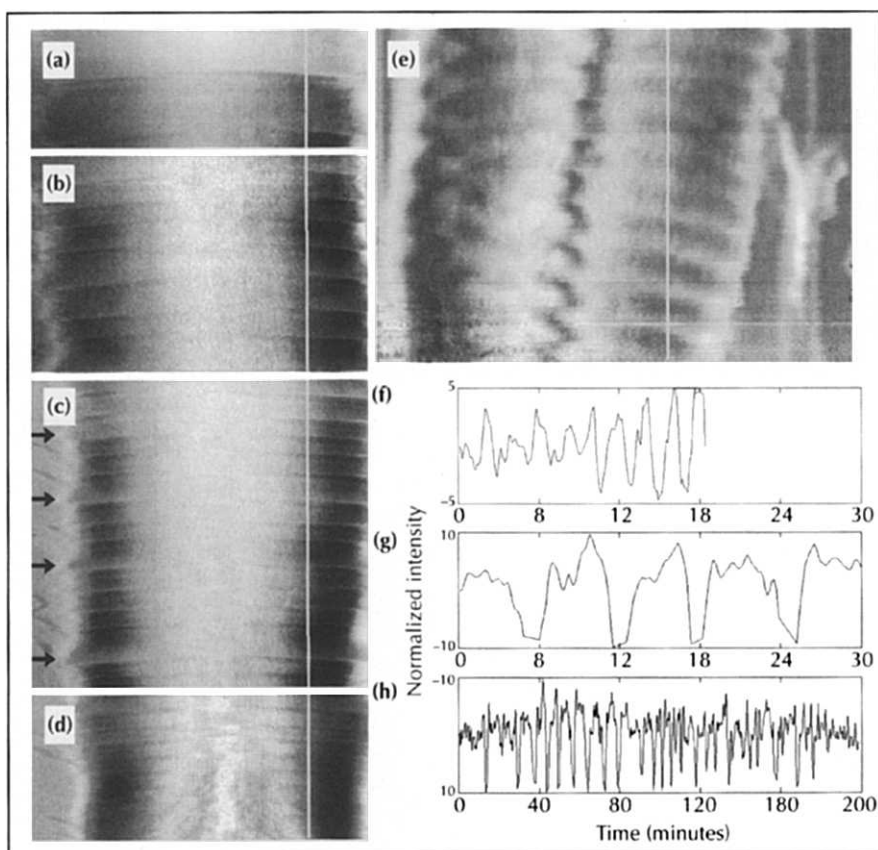
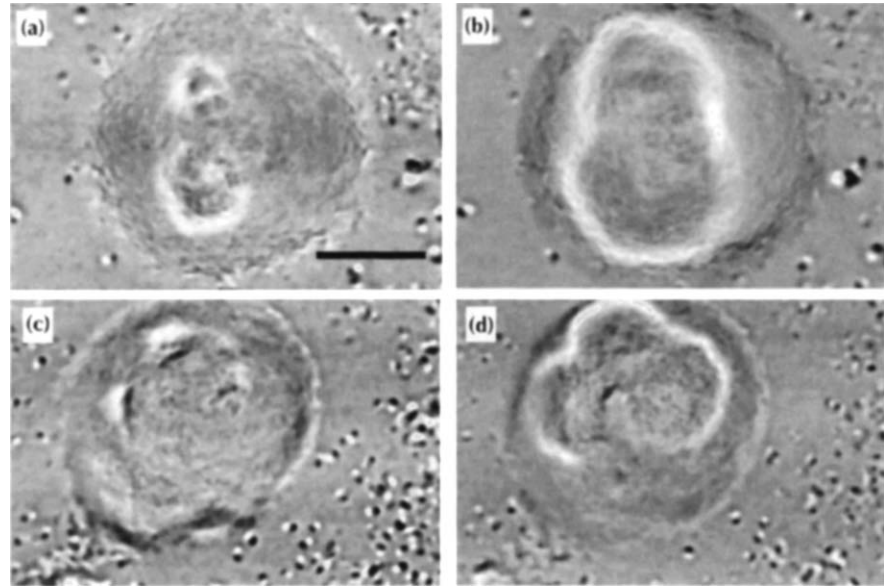


**Fig. 4.** Time-space plots of wave propagation. (a–d) Time-space plots observed in a XP55 mound, constructed as described in Fig. 3. As the sequence covers 3.5 h, the plots were acquired in four parts in order to refocus and adjust the forming mound. The intervals between the parts were less than 2 min, in which time the mound was refocused. The arrows in (c) indicate the appearance of strong contractions in-between regular ones. (e) Time-space plot of spiral waves in the streamer F mutant strain NP377. The plot covers a time period of 20 min. (f) Graph showing optical-density oscillations in strain NP377, analyzed from plot (e). (g) Oscillations in strain XP55, analyzed from plot (b). (h) Oscillations in strain XP55, analyzed from the plot sequence (a–d). Graphs were obtained by plotting the normalized and frequency-filtered intensity values [3] along a white, off-centre, vertical line in the time-space plots.

**Fig. 5.** Multiple pacemaker centres within a single mound. **(a,b)** Two autonomously oscillating centres shown at different time points (60 s apart) in strain XP55. **(a)** Wave propagation from two circular oscillating centres in a single mound. **(b)** The wavefronts extinguish each other at the location where they meet. **(c,d)** Three autonomously oscillating centres shown at different time points (60 s apart).



6b shows the same image after the continuous subtraction of five successive images. Clearly visible are five spiral arms, rotating counter-clockwise around a central core. The number of spiral arms was highly variable: we observed spiral centres with from two to ten arms rotating around the central core. The oscillation periods of multi-armed spirals occasionally dropped below one minute. We also observed spiral arms rotating in both directions, clockwise and counter-clockwise, in different mounds of the same population of cells. A three-dimensional representation of a three-arm spiral, observed in an AX-3 mound, is shown in Figure 6c.

#### Cell movement is opposite to signal propagation

Simultaneous observation of signal propagation (darkfield waves) and cell movement showed that cell movement was always opposite to the direction of signal propagation. Figure 6d shows an AX-3 mound under illumination conditions that allowed the visualization of cell movement. Figure 6e shows the corresponding cell-movement analysis by the velocity-vector method [12]: height represents cell-movement speed, and the vector field indicates the direction of cell movement. In the case of expanding

concentric ring waves, cell movement was always directed towards the organizing centre. In the case of spiral wave propagation, cell movement was counter-rotational. The two modes of cell movement differed in velocity — rotational cell movement was several times faster than cell movement straight towards the centre (Table 1). In mounds organized by concentric ring signals, cells often stayed in place for 30 minutes. More complex modes of cell movement were observed in mounds organized by two or more centres. In some cases, two centres showed counter-rotational cell movement; in other cases, groups of cells changed trajectories and moved to another centre, resulting in winding trajectories.

## Discussion

#### Darkfield waves in mounds represent the cAMP signal

We were able to observe waves of chemotactic activity under darkfield illumination in aggregation centres and mounds. These waves appear as thin, propagating dark bands. It is likely that these bands were caused by a fast contraction (resulting in a lower refraction) of the cells upon stimulation with cAMP. It is well established that, during early aggregation, optical density waves are caused by cell-shape changes upon stimulation by cAMP. By correlating the cAMP signal, using isotope dilution-fluorography, with the optical signal, it has been demonstrated that the optical-density waves observed during aggregation represent the propagating cAMP signal [4]. As we could measure wave propagation continuously from late aggregation until tip formation (over a period of 1–3.5 hours), we conclude that the observed wave pattern represents the propagating cAMP signal. The geometry of the propagating cAMP signal was strain specific: in strain XP55 we identified mainly concentric ring waves, whereas in two other strains, the streamer F mutant NP377 and the axenic strain AX-3, spirals with one or more arms predominated.

**Table 1.** Wave propagation in XP55 and AX-3 mounds.

Strain	XP55 (n = 10)	AX-3 (n = 8)
Predominant wave shape	Circular	Multi-armed spiral
Direction of movement	Towards centre	Rotational
Signal propagation velocity*	59 ± 15	111 ± 28
Cell movement velocity*	3.1 ± 0.4	17.7 ± 5
Oscillation period†	5.7 ± 2.5	2.8 ± 0.7

\*Velocity measured in  $\mu\text{m}$  per minute.  
†Period measured as minutes between oscillations.

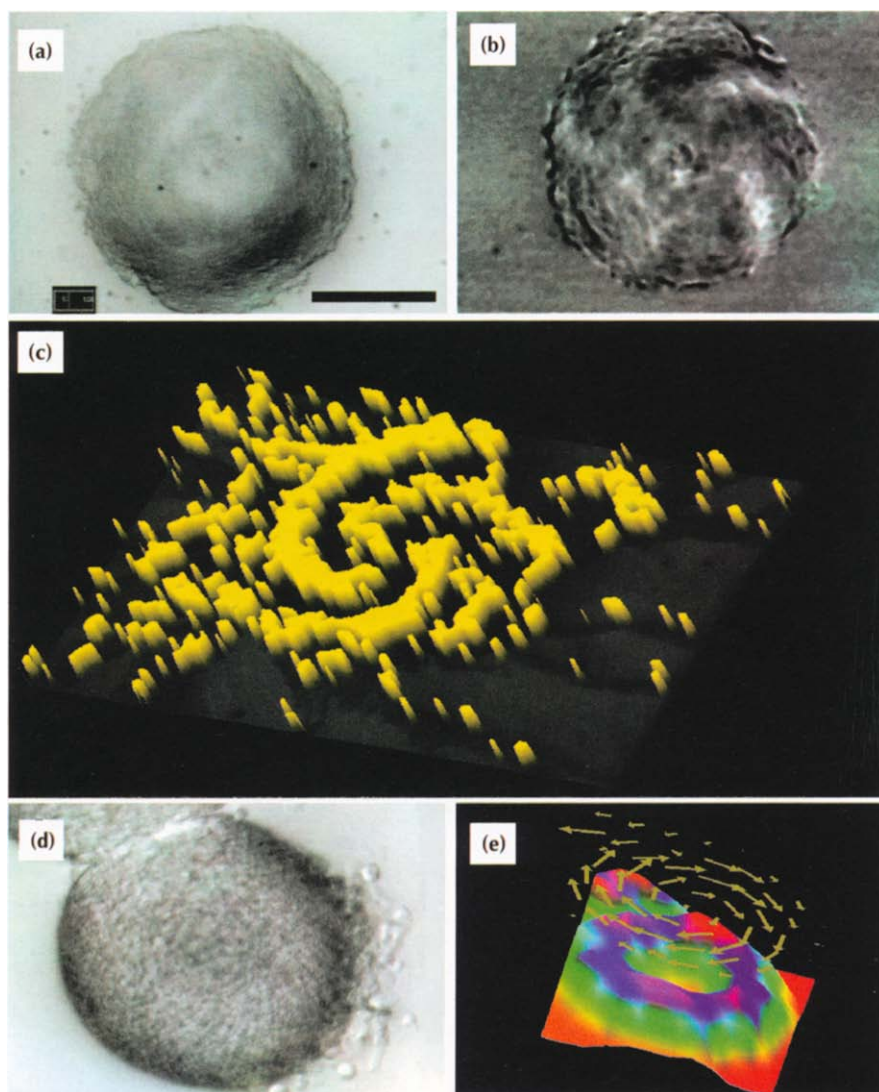


**Fig. 6.** Multi-armed spirals in mounds. **(a)** Darkfield image of an AX-3 mound. Scale bar = 100  $\mu\text{m}$ . **(b)** Five-armed spiral in the mound shown in (a), detected by image subtraction (see Fig. 3). Bright grey pixel values indicate the position of the wave front of the optical density waves, which cannot be observed in a single video frame (for better visibility, the waves are displayed in bright instead of dark pixel values). **(c)** Three-dimensional representation of a three-armed spiral measured in strain AX-3. Cell streams are still entering the aggregate. **(d)** Darkfield image of another AX-3 mound. **(e)** Velocity and direction of cell movement of the mound shown in (d). The method is described in [12]. Cell-movement velocity is displayed as a contour landscape. Faster velocities are represented by increased height and blue/purple pixels. The direction of cell movement is displayed as a vector field. Note the low movement speed in the centre of the mound.

### Complex signals in mounds

Our experiments show that *Dictyostelium* mounds can be organized by a range of different wave-propagation modes. Chemotactic signalling appears to be both complex and flexible, as all wave-propagation modes resulted in the formation of a tip, which is necessary for further development. The diverse geometry of the signals also leads to variety of complex cell-motion patterns (see also [13]). The different, sometimes interchanging, patterns of wave propagation in mounds appear to be a consequence of strain-specific variations in generating and relaying the cAMP signal, or may be due to the uneven distribution of different cell types with variable excitability. At the mound stage, two different cell types — the prestalk and prespore cells — differentiate at random, as shown by the use of cell-type-specific reporter-gene constructs [7]. Prestalk cells are more excitable than other cells in the mound, and sort to the top of the aggregate in order to form a tip. This sorting process has been shown to involve chemotaxis in response to cAMP [14]. The selective accumulation of highly excitable prestalk cells in the tip adds an extra 'feedback loop', stabilizing the tip as the sole excitable centre in the mound. The

feedback between wave propagation and the composition of the excitable medium is an important feature of this biological system, ensuring both flexibility and stability. In this respect, it differs fundamentally from physical and chemical systems in which feedback between wave propagation and excitability has not been described [11].

We were not able to observe directly the origin of multi-armed spiral centres. This was because of the faint visibility of darkfield waves in mounds, and because the subtraction of images only yielded usable results in the best experiments. The vigorous counter-rotational cell movement impeded clear results in the image-subtraction procedure as both signals, wave propagation and cell movement, were detected. However, multi-armed vortices were always very evident in time-lapse video films. These films suggest that multi-armed spiral centres form by a coincidental capture of free wave ends by the central core of the principal spiral centre. We also observed many cells and groups of cells that were able to oscillate autonomously. In time-lapse recordings, mounds appeared like fountains, with waves of chemotactic activity arising like bubbles all over the mound. In such a situation, the

formation of free wave-ends is likely to occur by symmetry breaking of concentric ring waves or by the formation of spiral centres.

## Conclusions

Darkfield waves represent a propagating chemical signal to which *Dictyostelium* cells respond by chemotactic movement. We have analyzed such waves continuously from late aggregation through the mound stage and up to tip formation, and conclude that this chemotactic signal is cAMP. Furthermore, mounds can be organized by signals of different geometries and temporal dynamics; these differences must have a genetic basis as they are strain-specific. The visualization of chemotactic waves in mounds closes a gap in our understanding of the developmental cycle of *Dictyostelium discoideum*. Chemical waves are very evident during the early aggregation phase, and waves of coordinated chemotactic cell movement have been observed in slugs — the stage that immediately follows mound formation [15]. It has been proposed, on the basis of cell-movement studies, that three-dimensional scroll waves are the major organizing principle during the slug stage of *Dictyostelium* [16], although no direct visualization of these waves has been possible up to now. Based on all these observations, it now appears likely that chemical waves of cAMP organize the entire developmental sequence of *Dictyostelium*.

## Materials and Methods

### Strains and culture conditions

Experiments were performed with *Dictyostelium discoideum* strain XP55, streamer F mutant NP377 and the axenic strain AX-3. XP55 and NP377 cells were grown on agar plates inoculated with bacteria (*Klebsiella aerogenes*). AX-3 cells were grown on bacteria or in suspension culture in axenic medium according to standard procedures [17]. Mounds were obtained by placing a streak of spores in the middle of an agar plate inoculated with bacteria. The growth zone of dividing amoebae expanded to both sides of the streak. Just behind the growth zone, differentiation started and mounds could be observed continuously. Axenically-grown AX-3 were washed twice in KK2 buffer (20 mM KPO<sub>4</sub> pH 6.8) and resuspended in KK2 at a density of  $5 \times 10^6$  cells ml<sup>-1</sup>. 5 ml cells were allowed to settle on 1% KK2 agar plates. After 5 min, the excess liquid was removed and the plate air-dried for 10 min. Mounds were analyzed after incubation overnight at 18 °C.

### Microscopy and digital-image processing

The mounds were filmed with a CCD video camera (Sanyo VC 2512). The petri dishes, filled with nutrient agar, were placed on a Zeiss IM 35 inverted microscope equipped with a 6.3× plan objective. Illumination was adjusted by sliding the phase ring of the condenser partly in the light path to obtain low-angle light scattering. Digital-image processing was performed with a 486 66 MHz Personal Computer equipped

with 20 MB RAM, 1 GB hard disc and an Imaging Technology AFG digitizing board with a resolution of 768 × 576 pixels. Noise in the video frames was reduced by averaging 30 video images in real time (25 frames s<sup>-1</sup>) before storing the images on an optical disc recorder (Sony LVR 4000P). Time-space plots were stored on-line during the experiment and analyzed as described [3]. The velocity-vector method is described in [12]. To visualize optical-density waves in still images, image pairs, 25–60 s apart, were subtracted. This resulted in high-intensity values where the two images differed, and in low-intensity values at locations where they were equal or similar.

*Acknowledgements:* We thank C.N. David for helpful comments and discussions. This work was supported by the Deutsche Forschungsgemeinschaft (We 1127).

## References

- Devreotes PN: *Dictyostelium discoideum*: a model system for cell-cell interactions in development. *Science* 1989, **245**:1054–1058.
- Alcantara F, Monk M: Signal propagation during aggregation in the slime mould *Dictyostelium discoideum*. *J Gen Microbiol* 1974, **85**: 321–334.
- Siegert F, Weijer CJ: Digital-image processing of optical-density wave propagation in *Dictyostelium discoideum* and analysis of the effects of caffeine and ammonia. *J Cell Sci* 1989, **93**:325–335.
- Tomchik K, Devreotes P: Adenosine 3':5'-monophosphate waves in *Dictyostelium discoideum*: a demonstration by isotope dilution-fluorography. *Science* 1981, **212**:443–446.
- Durston AJ: Pacemaker activity during aggregation in *Dictyostelium discoideum*. *Dev Biol* 1974, **37**:225–235.
- Foerster P, Müller SC, Hess B: Curvature and spiral geometry in aggregation patterns of *Dictyostelium discoideum*. *Development* 1990, **109**:11–16.
- Williams JG, Duffy KT, Lane DP, McRobbie SJ, Harwood AJ, Traynor D, et al.: Origins of the prestalk-prespore pattern in *Dictyostelium discoideum*. *Cell* 1989, **59**:1157–1163.
- Rubin J, Robertson A: The tip of the *Dictyostelium discoideum* pseudoplasmodium as an organizer. *J Embryol Exp Morphol* 1975, **33**:227–241.
- Futrelle RP, Traut J, McKee WG: Cell behavior in *Dictyostelium discoideum*: preaggregation response to localized cyclic AMP pulses. *J Cell Biol* 1982, **92**:807–821.
- Newell PC, Liu G: Streamer F mutants and chemotaxis of *Dictyostelium*. *Bioessays* 1992, **14**:473–479.
- Winfree AT: *When Time Breaks Down*. Princeton: Princeton University Press; 1987.
- Siegert F, Weijer CJ, Nomura A, Miike H: A gradient method for the quantitative analysis of cell movement and tissue flow and its application to the analysis of multicellular *Dictyostelium* development. *J Cell Sci* 1994, **107**:97–103.
- Doolittle KW, Reddy I, McNally JG: 3D analysis of cell movement during normal and myosin-II-null cell morphogenesis in *Dictyostelium*. *Dev Biol* 1995, **167**:118–129.
- Traynor D, Kessin RH, Williams JG: Chemotactic sorting to cAMP in the multicellular stages of development. *Proc Natl Acad Sci USA* 1992, **89**:8303–8307.
- Siegert F, Weijer CJ: Three-dimensional scroll waves organize *Dictyostelium* slugs. *Proc Natl Acad Sci USA* 1992, **89**:6433–6437.
- Steinbock O, Siegert F, Müller SC, Weijer CJ: Three-dimensional waves of excitation during *Dictyostelium* morphogenesis. *Proc Natl Acad Sci USA* 1993, **90**:7332–7335.
- Sussmann MM: Cultivation and synchronous morphogenesis of *Dictyostelium* under controlled experimental conditions. In *Methods in Cell Biology* 28. *Dictyostelium discoideum: Molecular Approaches to Cell Biology*. Edited by Spudich J. New York: JA Academy Press; 1987:9–29.

Received: 18 April 1995; revised: 5 June 1995.

Accepted: 15 June 1995.